An active wavefront sensor to make feasible adaptive optics on 100m class telescopes

Marco Xompero [a, 1], Carmelo Arcidiacono[b], Roberto Ragazzoni[c,d], Elise Vernet[c]
[a]Università di Padova, Dipartimento di Ingegneria;
[b]Università di Firenze, Dipartimento di Astronomia e Fisica dello Spazio;
[c]Osservatorio Astrofisico di Arcetri;
[d]Max Planck Institut für Astronomie – Heidelberg

ABSTRACT

Layer Oriented wavefront sensors can be made with a reasonable compact detector by the adoption of several stars enlargers, increasing only locally the focal ratio on the reference stars. The main opto-mechanical requirement in this kind of device is represented by the tolerances in tip and tilt of these star enlargers, which have to be moved over the Field Of View and aligned with the reference stars. A differential tip-tilt among the star enlargers leads to a mismatch between the different pupil images related to the reference stars. This misalignment eventually translates into a blurring of the measured wavefront, reducing the sensing quality. We describe a conceptual layout for an active control of the wavefront sensor, in order to reach the best mechanical positioning of these stars enlargers. In particular we discuss an algorithm to determine the effective pupils positions by simple movements and apply the requested displacement through commercially available piezoelectric actuators, shown in a preliminary opto-mechanical design of such wavefront sensor.
Keywords: AO, MCAO, Layer Oriented, 100m Telescopes, Ground Layer, Sub-pixel Alignment

1. INTRODUCTION

In order to avoid the atmosphere effect on science images adaptive optics systems have been implemented on most astronomical telescopes. Classical Adaptive Optics (AO) systems correct typically only a small fraction (few arcsec) of Field of View[1] centred on the wave-front sensor (WFS) reference used to drive the Deformable Mirror (DM). Beckers[2,3] introduced the Multi-Conjugate Adaptive Optics (MCAO) concept to expand the correction to larger FoV (1-2arcmin), using several DM conjugated to layers at different altitudes and several WFS looking to more references. The correction to apply to each DM can be computed in several ways analysing the information retrieved by the WFS. The tomography concept, also called Star Oriented (SO), introduced by Tallon and Foy[4], gives a solution to numerically disentangle the turbulence at fixed altitudes, through the classical WFS like Shack-Hartmann or Curvature. Then Ragazzoni and Marchetti and Rigaut[5] propose the concept of modal tomography, where the layers reconstruction is performed in a modal way. The efficiency of this approach has been tested on the sky[6], although in a preliminary form. At the same time a new concept, called Layer-Oriented[7,8] (LO) on the perspective to apply it on 2nd generation telescopes. In this approach all the guide stars are simultaneously sensed by one WFS for each conjugated plane. The phase measurements of each WFS are used to compute the correction to apply to the DM conjugated at that layer. Each DM and WFS couple works in a hardware independent closed-loop way with a small consuming of computer power to calculate the correction with respect to the SO approach. A natural sensor for the LO approach is the pyramid WFS[9], in which each guide star is focused on the vertex of a pyramid in order to project on the sensor four images of the pupil. The main opto-mechanical requirements are the tip and tilt tolerances of the star enlargers which have to be aligned with the reference stars. A differential tip tilt among the star enlargers (SE) leads to a mismatch between the different pupil images on the ground WFS plane. The misalignement translates into a blurring of the phase measurements with a loosing of the efficiency. In this paper we present an algorithm to make active the ground layer WFS and to achieve a strong pupils overlap in order to apply this approach on a Extremely Large Telescope as the Overwhemingly Large Telescope[10,11] (OWL), in section 2 we describe the algorithm structure and of each step. In section 3 we present a pupil

[1] Further author information:
M.X: E-mail: marco@arcetri.astro.it

model and the simulation parameters used to check the procedure. In section 4 we give the algorithm performance in terms of error on the pupils mismatch and time spent by the computing procedure to achieve the correct position of the star enlargers.

2. ALGORITHM DESCRIPTION

The goal of the algorithm is to correct the inclinations of all the star enlargers with accuracy under the limit of 1arcmin. We reach this result by centring all the pupils projected by the SE-pyramids on the ground layer WFS. In this way the star enlargers will be automatically aligned to the optical axis of the overall adaptive system.
We design a closed loop procedure to compute and to correct the pupils centre positions of the references stars on the sensor. The main idea is to move simultaneously at different frequency the SE in order to shift the pupil images of the reference stars on the detector. In this way is possible to identify the single pupils and their positions by temporal filtering the frames recorded by the WFS. These movements are needed because the pupils are super-imposed and it is not possible to distinguish among them using only a single frame image. The direction and the frequency of the movement are two critical issues for the identification of the different pupils and their geometrical centres.

2.1. Block Diagram

In the following we describe the main architecture of the algorithm, as it is supposed to be applied during the MCAO initialization procedure.
We plan to set up the Real Time Computer (RTC) of the adaptive system to move the pyramids holders by a tip-tilt electrical device. While the stars enlargers are moving, the WFS detector conjugated to the ground layer records the images of the references stars pupils. In order to optimize the performance we apply a border pixels selection and the algorithm analyses the temporal variation as signal for each pixel of the detector taken into account. To these signals we apply a Discrete Fourier Transform: in this way the pixels relative to every frequency applied to the SEs movement are found. The power spectrum data of every pixel relative to each frequency are used to generate an array of weights, hereafter called “weight frame”. In this way we compute an array with the information available to identify the position of each references pupil and then about the star enlargers inclination with respect to the optical axis. We use those weight frames to find the position of the pupil centre on the detector area and then to send the corrections for the SE to the RTC. This algorithm is developed to work in closed-loop, in order to improve the rejection error on centres identification and the bad mechanical positioning. A block diagram describing the different algorithm steps is given in Figure 1.

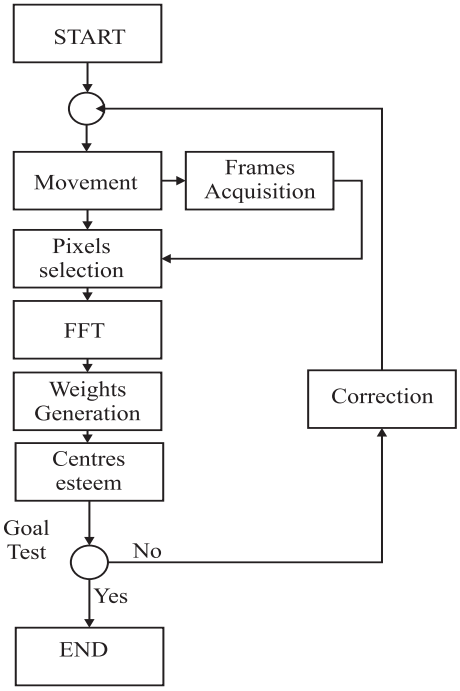

Figure 1. Block diagram of the mains algorithm steps.

2.2. The star enlargers movement

We suppose that each star enlarger is able to move in a circular way around its axis. This movement produces a circular shift of the pupil on the detector of 3.5 pixels radius. Of course, the RTC should be able to reposition the SE at the same starting point. Each pyramid shift is a combination of a sinusoidal and a co-sinusoidal movement with the same amplitude and frequency and these are different for each pupil. We selected equally spaced frequencies between 10 and 20 Hz, rounded according to the DFT sampling. The sampling rate chosen is 50 Hz range binned by 1024 steps. Therefore we shift all the frequencies of five samples, in order to avoid the sub-harmonic interferences that we find in the spectral analysis at 10 and 15 Hz.

Pupil	1	2	3	4	5	6	7	8	9	10	11	12
Freq	10.25	11.08	11.91	12.74	13.57	14.40	15.23	16.06	16.89	17.72	18.55	19.43

Table 1. Here are listed the frequencies, in Hz used in the simulations. We use the floating point values but in the table we report here the approximation.

2.3. The pixels selection

The computation time is a critical factor for every algorithm. This goal is achievable optimising the selection of the pixels where the FFT will be computed. The effect of the not correct superposition of the pupils is more evident at the borders of the illuminated region on the CCD (the border of the metapupil projected of the ground WFS). Here the variation of intensity due to the SE movements is more evident and then we apply the Fourier transform to these border pixels only in order to speed up the computation procedure. To select these pixels we use a frame acquired when the pupil movements are not started yet and we smooth this image, using a simple convolution with a normalized bi-dimensional Gaussian characterized by a standard deviation of 8 pixels. Thus we set up the application of the Sobel edge detection algorithm, which performs a 2D gradient by a convolution with a short square matrix and then we compute the binary conversion bounding on the resulting frame. Through this procedure we obtain the mask of the pixels to be used for the computation of the pupil centres. We set the threshold to 1/3 of the maximum frame value for the Sobel procedure, but this value could be changed in order to increase or to decrease the amount of data, the computation time and the accuracy of the following steps.

Figure 2. Example of pixel selection mask.

2.4. The weights frames generation

The algorithm uses only the data relative to the pixels identified by the selection described before (ad example the white pixels in the mask in figure 2). For each pixel we consider the temporal signal given by the intensity variation recorded in the 1024 frame taken by the ground WFS during the movements of the SE. It is clear that the edge pixels are the most important for our scope. The temporal series relative to every pixel selected are the input data for the Discrete Fourier Transform computed very efficiently by the FFT algorithm. The result is a new set of signals which give us useful information: first of all, we are able to identify the pixels that clearly belongs to one pupil or to another one by simply looking at the peaks of the power spectrum, and, second, we are able to verify the quality of this measure by comparing those peaks values with the noise level. Nevertheless we modify this approach: initially we decide to take the values of the DFT at the known frequencies applied to the movements, into a range of one sample around the exact value, then, in order to correct for noise pollution these values, we subtract to them the noise mean retrieved by the remaining dots. The peaks higher than a threshold of 4 times the noise standard deviation are considered exact, while the others are set to the noise mean. For each frequency a new frame is generated: it is composed by the map of the power spectrum values found by the FFT at that specific frequency.

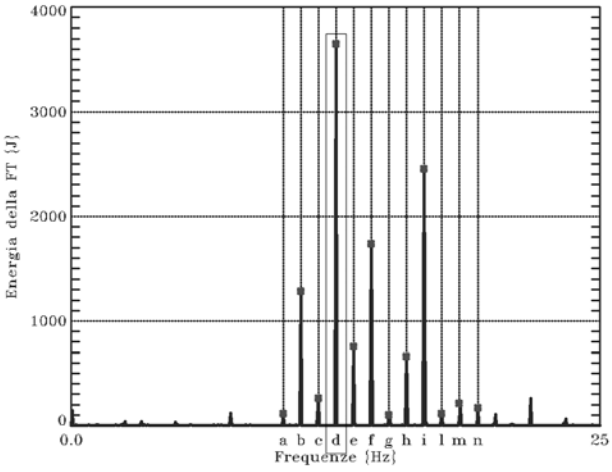

Figure 3. In this picture is plotted an example of DFT and peaks retrieval, used in the simulation.

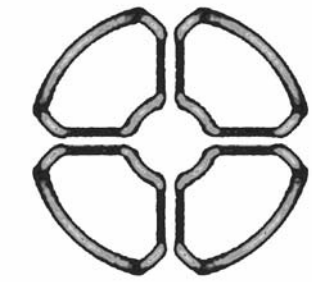

Figure 4. Here is shown an image of a weights frame array used in the simulations.

2.5. The centres assessment

The good centres assessment is a crucial point for the reliability of the algorithm. To solve this problem we decide to fit on each pupil weights frame a circle with a fixed diameter of 100 pixels and centre coordinates as free parameters (see figure 5). The high relative values differences in the same frame due to the pupil edge pixels presence helped us to obtain very good evaluation. However, this first evaluation is not good enough to reach an RMS error on the centres position lower than 0.1 pixels (considering the 12 pupils), in the case of poor estimated weights. So we apply a recursive fitting: in first instance we roughly find the centres with an initial identification and then the algorithm try to exclude from the fitting procedure those pixels which distance from the circumference is too high (ad example more than 10 pixels as cutting value). Of course these pixels are not considered yet in following iterations. For each iteration this distance decreases and the process stops when a threshold of 5 pixels is reached or if the parameter value never changed in the last 20 iterations. This approach allows improving the centres position assessment error and moreover it increases the precision on the positioning. Even if the initial centres evaluations are poor and the first corrections performed are not exact, in the following iterations the parameter identification becomes more and more accurate, finally achieving an assessment values ≈0.03 pixel RMS at the final iteration.

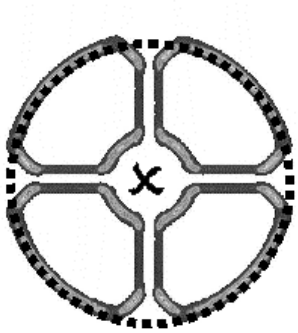

Figure 5. Here are plotted a fitting example and center estimation.

3. SIMULATION PARAMETERS

We tested the performances of the algorithm described above developing a numerical code that simulates the effect of the SE movements on the pupil imagined on the detector of the ground layer WFS. It starts simulating the pupil displacing due to the error in the inclination of the SEs and the measurements produced by the WFS, it applies the algorithm and the corrections. Starting from the positions computed this procedure simulates a new circular shift of the pupils relative to each SE and correcting again for the shifts estimated until the error goes under the 0.1 pixel shift (RMS) for all the pupils.

3.1. Metapupil simulation

We suppose that for the ground layer WFS for an OWL-like telescope each pupil will be sensed by a square array of 1024×1024 CCD pixels. Because of the huge number of pixels we decide to simulate the system considering each pupil image as projected on a CCD camera of the ground layer WFS with 100 pixels diameter centred over a grid of 128 by 128 pixels (that gives a pixel scale of 1m/px for the 100m OWL pupil). The pupil presents the shadow of the central circular obstruction and of the 4 spiders of the secondary mirror. The radius of the central obstruction is about 30 pixels and the spider arms size is large 4 pixels and 24 pixels in the external part (see figure 6). We consider as many pupils as references (12), taking into account the photon flux at the sensing pass-band of each stars and the partial illumination of the pixels on the pupil limits. To each pupil intensity-map is added the contribution of the Poissonian photon noise, generated by a Gaussian distribution with standard deviation σ_n :

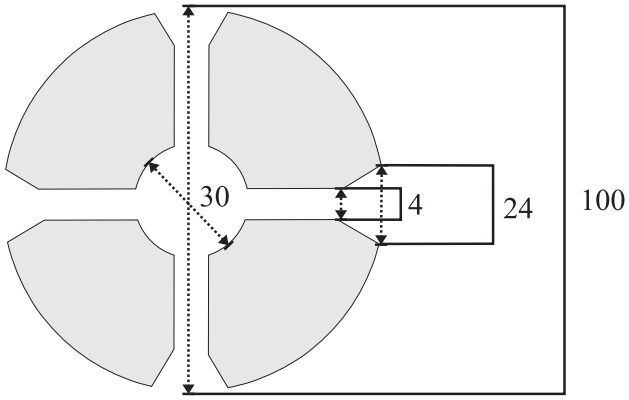

Figure 6. Size of the pupil used for the simulations.

$$\sigma_n = \sqrt{N_{photons}}$$

where $N_{photons}$ is the number of photons collected on each pixel (taking into account the re-size used for the simulation purposes from 1024×1024 to 128×128 pixels) coming from the reference star. In order to simulate the ground layer metapupil we overlap all the pupils considering a random displacing among the centres of $3\sqrt{2}$ pixels amplitude with a linear interpolation for the non integer pixel shift. We take also into account the read-out noise of the detector by adding to the frame a white noise of standard deviation $\sigma_{RON} = 3e^- / frame$.

3.2. Others important parameters

For the algorithm computation we also need to define other parameters regarding the sensor characteristics. We chose a WFS wavelength of 600nm for the photons acquisition and a bandwidth of 500nm. The magnitudes of the selected stars have random value between 17.2 and 18.2 (as in the cited paper[12]). We analyse the effects of several integration time applied to the WFS on the achievable performances and we find out that at least 30 ms of integration time are needed to achieve the scope. The total number of frames that we chose to use is 1024, giving a total frames acquisition-time of about 30 seconds. The twelve pupils must have their centres positioned at less than 0.1 pixels RMS from the alignment axis. We chose this requirement by considering the case of a real implementation with at least a grid of 1024×1024 pixels. We considered a typical good Fried parameter, r_0 = 20cm (at the sensing wavelength). This r_0 is fitted by a 2 pixels side square on the 100m pupil sampled with 1024×1024 pixels. We supposed that the misalignment effect is negligible in the local tip-tilt assessment if its value is at least 10 times less than the Fried parameter mapped dimension.

Real grid size (Pixels)	1024×1024
Simulated grid size (Pixels)	128×128
Real pupil diameter (Pixels)	800
Sim. pupil diameter (Pixels)	100
WFS λ (nm)	600
Bandwidth (nm)	500
Magnitude	17.2-18.2

Number of pupils overlapped	12
Max displacement (Pixels)	3.5
Number of frames N	1024
RMS range alignment (Pixel)	0.1
Integration time (ms)	30
Read-out noise	$3e^-$
Poissonian noise	Yes

Table 2. In these tables are listed the main characteristics of the simulated sensor and of the simulation performed to test the algorithm.

4. ALGORITHM PERFORMANCES

The critical parameters in the procedure were represented by the magnitude of the stars, the integration time and by the WFS wavelength and bandwidth. The reference stars magnitude is an effective given data and integration time is a free parameter while the others two are building bounds. The key point to achieve good performance is represented by the intensity of the light on the WFS. With faint stars (mag>18-19) is possible to achieve good performances simply increasing the integration time but this translates in a longer overall time to reach the closure. The stability of the algorithm in a closed loop way is largely dependent from the identification characteristics: in our simulations, the centre assessment error was smaller than 0.5 pixels RMS and so in each iteration the system moves to correct the pupils but always within the 0.1 pixel RMS range. The identification error has also the characteristics to decrease more and more, proportionally to the aligning of the pupils and it cancels out the possibility to have instable behaviours. To evaluate the algorithm performances we used the radius of gyration with respect to the aligning axis considering each centre as a unitary mass. The gyration radius and the pupils position are stable just at the third iteration and they vary below their threshold value. In average for each iteration about 18s are needed and the fixed time necessary to take the frames was about 30s. Therefore we can say that with an approximate overall time smaller than 3 minutes we can actively correct the misalignment of the SE by using the ground layer pupils.

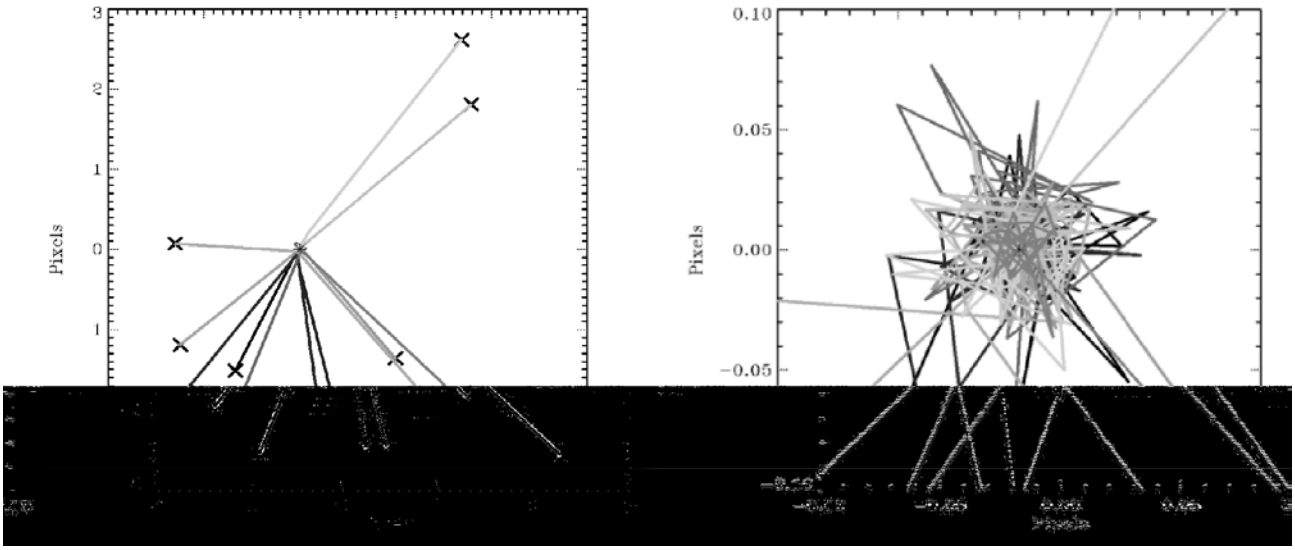

Figure 7. These 2 plots show the positions of the 12 pupils from the starting point to the 30-th iteration of the active loop: normal view on the left and zoomed on the right. The crosses represent the canters position and the solid lines the shift. (Different grey colors for different pupils)

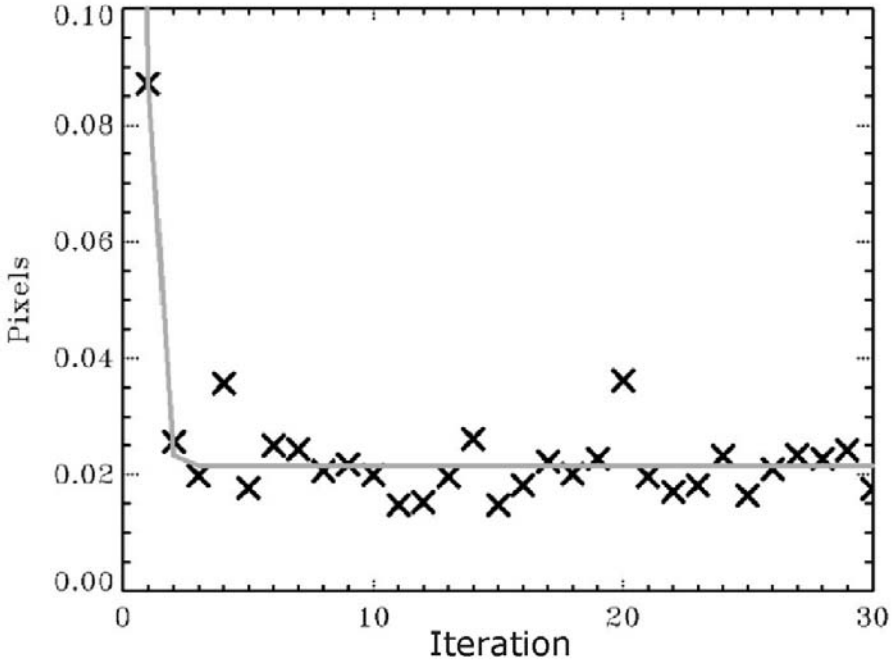

Figure 8. Radius of gyration. In this plot to the simulated data (crosses) is super-imposed the exponential fit in order to show the stability of the algorithm.

5. CONCLUSIONS

We analysed the case of a Layer-Oriented approach for a 100m-class telescope as OWL and especially the pupil alignment problem. Therefore we developed a software solution to this crucial problem that use the ground layer WFS of the adaptive system in an active way for the correct axis positioning of the star enlargers. In the simulations the problem was re-scaled reducing the pupil size with respect the real case but preserving the same characteristics (from 1024×1024 to 128×128). A procedure to perform an optimal selection of the pixels useful for the alignment is here described. The frequency set has been chosen in order to optimize the identification quality of all the pupils simultaneously. We have pseveral parameters in roder <"order to achieve a good centres estimations step that increases the ability of the algorithm to retrieve the real pupils position according to the star enlargers alignments reached. The algorithm works in a closed loop way in order to improve the stability and the errors rejection. The performances of the procedure described here were tested by simulations, in particular we considered a case close to the OWL Layer Oriented simulations discussed elsewhere[12], where the OWL LO-related performances are presented. However here we show a preliminary work: we have took into consideration the photon noise of the reference light but neglecting, at least in this first instance, the effects due to the turbulence that, is superimposed to the brightness variations due to the Poissonian photon noise. This is an effect that will deserve a study, but we just point out here that the typical realization time of our measurements (few tens of seconds) is longer than the coherence time of such atmospheric effect, so we expect a small lost of performances.

6. ACKNOLEDGEMENTS

Thanks are due to Mian A. for the useful discussion, to Diolaiti E. and Farinato J. for the development of this project and Lombini M. for the support.

7. REFERENCES

1. Beckers J. M., “Adaptive optics for astronomy – Principles, performance and applications”, ARA&A 31, pp. 13-62, 1993.
2. Beckers J. M., “Increasing the size of the isoplanatic patch size with multiconjugate adaptive optics”, in ESO conference on Very Large Telescopes and their instrumentation. M.H. Hulrich ed., pp. 693, 1988.
3. Beckers J. M.,, “Detailed compensation of atmospheric seeing using multiconjugate adaptive optics”, Proc. SPIE **1114**, pp.215-217, 1989.
4. Tallon, M. and Foy, R.”Adaptive telescope with laser probe : isoplanatism and cone effect”, A&A, **235**, p.549-557, 1990.
5. Ragazzoni R., Marchetti E. and Rigaut F., “Modal tomography for adaptive optics”, A&A **342**, pp. L53-L56, 1999.
6. Ragazzoni R., Marchetti E. and Valente G.,“Adaptive-optics corrections available for the whole sky”, Nature, **403**, pp. 54-56, 2000
7. Ragazzoni R., Farinato J., Marchetti E., “Adaptive optics for 100m-class telescopes: new challenges require new solutions”, Proc. of SPIE **4007**, pp. 1076-1087, 2000.
8. Ragazzoni R., “Adaptive optics for giants telescopes: NGS vs. LGS”, in ESO Proceedings of Bäckaskog Workshop on ELTs, T. Andersen, A. Arderberg and R. Gilmozzi eds., pp. 175-180, 2000.
9. Ragazzoni R., “Pupil plane wave front sensing with an oscillating prism”, J.of Mod.Opt., **43**, pp. 289-293, 1996.
10. Gilmozzi R., Delabre B., Dierickx P., Hubin N., Koch F., Monnet G., Quattri M., Rigaut F., Wilson R.N., “Future of fille aperture telescopes: is a 100m feasible?”, Proc. SPIE **3352**, pp. 778-791, 1998.
11. Dierickx, P. and Gilmozzi, R., “OWL concept overview”, Proceedings Bäckaskog Workshop on Extremely Large Telescopes (Eds T. Andersen, A. Ardeberg, R. Gilmozzi), p 43, 2000.
12. Fedrigo E., Marchetti E., Arcidiacono C. and Diolaiti E., “Layer Oriented single and dual field-of view performance for OWL” , Proc. SPIE **4840**, pp. 415-426, 2003.